Ways to improve RAIM/AAIM availability using position domain performance computations

P.B. Ober
Delft University of Technology
Telecommunications and Traffic Control Systems Group
Mekelweg 4, 2628 CD Delft, The Netherlands

BIOGRAPHY

Bastiaan Ober has 4 years of experience in the field of radio navigation. He received his M.Sc. in Electrical Engineering from Delft University of Technology in 1993. His thesis treats the fast computation of integer ambiguities for carrier phase GPS with the basis reduction method. Further areas of experience include the influence of multipath on GPS positioning, carrier phase differential GPS, and integrity of GPS and integrated navigation systems. He is currently working as a Ph.D. student at Delft University of Technology, The Netherlands, doing research on the design of optimal integrity monitoring algorithms for integrated navigation systems.

ABSTRACT

This paper discusses the performance of RAIM/AAIM in terms of the probabilities of missed and false detection of a *position error* of the navigator. The statistical independence of position error and test statistic is exploited to compute missed and false detection probabilities from the distributions of position error and test statistic straightforwardly.

We compute exact probabilities and computationally less involved approximations, as well as the probabilities that are obtained when using a conventional method [Leva96] that works in the measurement rather than the position domain. The results of the latter prove to be too pessimistic, and will therefore result in reduced RAIM/AAIM availability. We also show that representing the measurement geometry by the worst integrity measurement only, as is often done, is disadvantageous with respect to RAIM/AAIM availability.

1. Introduction

The goal of this paper is to show how the performance of Receiver or Aircraft Autonomous Integrity Monitoring (RAIM/AAIM) algorithms can be computed in terms of the probabilities of missed and false detection of a *position error* of the navigator, and how exact computations of these probabilities can be used to get a higher RAIM/AAIM availability compared to the conventional method of [Leva96].

After introducing the measurement model in section 2, position and noise estimation are discussed in section 3. Section 4 describes the formulation of the position error detection problem as a test between two hypotheses, and shows how to compute the probabilities of missed and false detection. Section 4.4 compares the formulation of this paper to current navigational practice, and outlines which assumptions are often made, and when these are violated. Computer computations with GPS constellations are presented in section 5. Finally, in section 6, we summarize the main conclusions that can be drawn from the results of these computations.

2. The system model

In this paper, we will assume that the relation between the measurements that the navigation system provides, and the actual position of the user, is given by an overdetermined linear regression model:

$$\vec{z} = H \cdot \vec{x} + \vec{v} \tag{2.1}$$

in which:

$\vec{z}$: n-vector of measurements
H : $n \times m$ observation matrix
$\vec{x}$: m-vector of unknowns (usually position, clock bias)
$\vec{v}$: n-vector with independent noise and biases in the measurements

with $n > m$.

The vector of unknowns will be called 'position', although it might contain other unknowns as well. The noise in (2.1) is assumed to be normally distributed with mean $\vec{\mu}_v$ and covariance R_v:

$$\vec{v} \sim \mathsf{N}\left(\vec{\mu}_v, R_v\right) \qquad (2.2)$$

We will refer to a nonzero mean noise $\vec{\mu}_v$ as *measurement bias*, and to a nonzero mean position error $\vec{\mu}_{\Delta\hat{x}}$, to be defined in (3.7), as *position bias*. The weighted norm of a vector $\vec{y}$ will be denoted and defined by:

$$\left\| \vec{y} \right\|_{R_y^{-1}}^2 = \vec{y}^T R_y^{-1} \vec{y} \qquad (2.3)$$

Usually the weightmatrix R_y^{-1} is the inverse of the co-variance of $\vec{y}$.

3. Position and noise estimation

The model (2.1) has two unknowns: the position and the momentary value of the measurement noise. In this section we will show, how both can be estimated from the measurements.

When (2.2) holds, it is well known [Rao95] that the best (minimum covariance) linear estimation of the position is given by the weighted least squares solution of (2.1):

$$\hat{\vec{x}}_{LS} = N\vec{z} \qquad (3.1)$$

with

$$N = (H^T R_v^{-1} H)^{-1} H^T R_v^{-1} \qquad (3.2)$$

This estimation is normally distributed:

$$\hat{\vec{x}}_{LS} \sim \mathsf{N}\left(\vec{\mu}_{\hat{x}}, R_{\hat{x}}\right) \qquad (3.3)$$

with mean and covariance:

$$\vec{\mu}_{\hat{x}} = \vec{x} + N\vec{\mu}_v \qquad (3.4)$$

$$R_{\hat{x}} = (H^T R_v^{-1} H)^{-1} \qquad (3.5)$$

Instead of using the position (3.3) itself, it is often more convenient to use the distribution of the position *error*, that is just a shifted version of (3.3) and is therefore normally distributed as well:

$$\Delta\hat{\vec{x}}_{LS} = \hat{\vec{x}}_{LS} - \vec{x} \sim \mathsf{N}\left(\vec{\mu}_{\Delta\hat{x}}, R_{\Delta\hat{x}}\right) \qquad (3.6)$$

with

$$\vec{\mu}_{\Delta\hat{x}} = N\vec{\mu}_v \qquad (3.7)$$

$$R_{\Delta\hat{x}} = (H^T R_v^{-1} H)^{-1} \qquad (3.8)$$

The linear model (2.1) can be seen as a decomposition of the measurement vector $\vec{z}$ into a deterministic part $H\vec{x}$ and a stochastic part $\vec{v}$. When we remove the estimated deterministic part, we obtain the best estimation of the noise vector, usually named the *least squares residual*:

$$\hat{\vec{v}}_{LS} = D\vec{z} \qquad (3.9)$$

with

$$D = I - H(H^T R_v^{-1} H)^{-1} H^T R_v^{-1} = I - HN \qquad (3.10)$$

The residual is normally distributed

$$\hat{\vec{v}}_{LS} \sim \mathsf{N}\left(\vec{\mu}_{\hat{v}}, R_{\hat{v}}\right) \qquad (3.11)$$

with mean and covariance

$$\vec{\mu}_{\hat{v}} = D\vec{\mu}_v \qquad (3.12)$$

$$R_{\hat{v}} = DR_v D^T \qquad (3.13)$$

Note that both the position and the noise estimation are unbiased when the measurements are unbiased, that is, when $\vec{\mu}_v = \vec{0}$.

4. Availability, position error detection and hypothesis testing

The required navigation performance (RNP) parameters specify the maximum allowable position error for a certain phase of flight. We will denote this error by $RNP_{\Delta\hat{x}}$. A navigation system has sufficient integrity when users can detect too large a position error with sufficiently high probability. Although not a safety matter, it is also important that the system does not give too many false detections.

The detection problem is usually formulated as a test between two hypotheses. Assuming that the position co-ordinates are defined in an orthonormal (Cartesian) frame, we would like to be able to distinguish between

$$H_0 \ (no \ error)\colon \left\| \Delta\hat{\vec{x}}_{LS} \right\|^2 \le RNP_{\Delta\hat{x}}^2 \qquad (4.1a)$$

and

$$H_1 (error): \quad \left\| \Delta \hat{\bar{x}}_{LS} \right\|^2 > RNP_{\Delta \hat{x}}^2 \qquad (4.1b)$$

by use of some test statistic. Unfortunately, the position error is not observable. All we can do is to use the least squares residual (or, equivalently, a parity vector) instead. As can be seen from (3.7) and (3.12), measurement biases generally increase both the position error and the residual, and it is this relationship that can be exploited. Therefore, a suitable choice for the test statistic is the Sum of Squared Errors, that is nothing but the normalized squared norm of the least squares residual:

$$SSE = \left\| \hat{\bar{v}}_{LS} \right\|_{R_v^{-1}}^2 = \hat{\bar{v}}_{LS}^T R_v^{-1} \hat{\bar{v}}_{LS} \qquad (4.2)$$

In case of a large measurement bias, both position bias and SSE will become large, and therefore the 'no error' hypothesis is only accepted when SSE remains below a certain threshold:

$$SSE \le SSE_{threshold} \Rightarrow H_0 \ is \ accepted$$
$$SSE > SSE_{threshold} \Rightarrow H_1 \ is \ accepted \qquad (4.3)$$

When we use the decision criterion (4.3) it can happen that we take a wrong decision and accept the wrong hypothesis. The two possible errors that can be made are called missed detection (accepting H_0 unjustly) and false detection (accepting H_1 unjustly).

Because the test statistic and position error are statistically independent (see appendix A for a proof), the probability of missed detection (P_{MD}) can simply be expressed as the product of the probabilities of *no detection* and *position error*. Similarly, the probability of false detection (P_{FD}) is the product of the probabilities of *detection* and *no position error*:

$$P_{MD} = (1 - P_{detection}) \cdot P_{pos\_error}$$
$$P_{FD} = P_{detection} \cdot (1 - P_{pos\_error}) \qquad (4.4)$$

in which the following notations are introduced:

$$P_{pos\_error} = P(\|\Delta \hat{\bar{x}}_{LS}\|^2 > RNP_{\Delta \hat{x}}^2)$$
$$P_{detection} = P(SSE > SSE_{threshold}) \qquad (4.5)$$

A navigation system is only available when the probabilities of missed and false detection remain below the values that are specified by the RNP parameters. To know if the system is available or not, we need to compute these missed and false detection probabilities. We will deal with this computation in the remainder of this chapter. First of all, we need the distributions of position

error and test statistic. These distributions are discussed in section 4.1 and 4.2. Unfortunately, they both depend on the unknown measurement bias. Section 4.3 will show how to deal with this problem by means of a worst case approach. In 4.4 we will shortly discuss the way navigation literature usually determines the missed and false detection probabilities. We outline the assumptions that are commonly made, and indicate when these are violated.

4.1 The distribution of the test statistic

The test statistic *SSE* is a *normalized* noncentral quadratic form in normal variables. As has been described extensively in RAIM literature, see for example [Brown96], it has a noncentral chi-square distribution with *n-m* degrees of freedom and a noncentrality parameter λ_{SSE}:

$$SSE \sim \chi^2(n - m, \lambda_{SSE}) \qquad (4.1.1)$$

with

$$\lambda_{SSE} = \vec{\mu}_v^T D^T R_v^{-1} D \vec{\mu}_v = \vec{\mu}_{\hat{v}}^T R_v^{-1} \vec{\mu}_{\hat{v}} \qquad (4.1.2)$$

As can be seen from (4.1.2) the noncentrality λ_{SSE} depends on the unknown measurement bias, as well as on the known measurement geometry that is reflected in D. The more favorable the geometry, the larger λ_{SSE} will become for a certain bias, and the easier it will be to detect it.

4.2 The distribution of the position error

Unlike the test statistic, the squared norm of the position error $\|\Delta \hat{\bar{x}}_{LS}\|^2$ is a *nonnormalized* noncentral quadratic form in normal variables:

$$\left\| \Delta \hat{\bar{x}}_{LS} \right\|^2 = \vec{v}^T N^T N \vec{v} \ \text{with} \ \vec{v} \sim \mathsf{N}(\vec{\mu}_v, R_v) \qquad (4.2.1)$$

for which we can define a noncentrality parameter similarly to (4.1.2) as

$$\lambda'_{\Delta \hat{x}} = \vec{\mu}_v^T N^T N \vec{\mu}_v \qquad (4.2.2)$$

The accent in (4.2.2) indicates that this noncentrality is not belonging to a chi-square distribution.

The distribution of (4.2.1) is discussed in great detail in [Johnson72]. Its probability density function is constant on all ellipsoids of the form [Tong90]

$$\left\| \Delta \hat{\vec{x}}_{LS} - \vec{\mu}_{\Delta \hat{x}} \right\|_{R_{\Delta \hat{x}}^{-1}} = c \ , \ c \geq 0 \qquad (4.2.3)$$

The RNP parameters require the position error to remain in the sphere given by

$$\left\| \Delta \hat{\vec{x}}_{LS} \right\| \leq RNP_{\Delta \hat{x}} \qquad (4.2.4)$$

The probability that the position error exceeds the required bounds is therefore described by the probability content of that part of the elliptical distribution that lies outside of the sphere (4.2.4). This situation is depicted in figure 1.

Appendix B indicates how the position error distribution can be computed. The exact distribution function proves to be computationally expensive and is hard to tabulate, because a total of $2m$ parameters is involved. Therefore, it makes sense to investigate how it could be approximated.

One possible approximation is described in [Lee95]. Lee uses the marginal distribution of that component of the position error that lies in the direction of the position bias, see figure 2. Clearly, this approach will always under-estimate the position error probability. Lee uses the same approximation for the test statistic as well, and thereby overestimates the 'no detection' probability. The product of both approximations can therefore become both larger and smaller than the actual missed detection probability. This also applies to false detections.

A second approach could be to use a normalized position error with a noncentral chi-square distribution. Geometrically, normalization results in the use of the probability content of spheres instead of ellipsoids, see figure 3. Algebraically, we use the fact that the position error and its normalized variant are related by

$$\frac{1}{\lambda_{\max}(R_{\Delta \hat{x}}^{-1})} \left\| \Delta \hat{\vec{x}}_{LS} \right\|_{R_{\Delta \hat{x}}^{-1}}^2 \leq \left\| \Delta \hat{\vec{x}}_{LS} \right\|^2 \leq \frac{1}{\lambda_{\min}(R_{\Delta \hat{x}}^{-1})} \left\| \Delta \hat{\vec{x}}_{LS} \right\|_{R_{\Delta \hat{x}}^{-1}}^2$$

$$(4.2.5)$$

where $\lambda_{\min}(R_{\Delta \hat{x}}^{-1})$ and $\lambda_{\max}(R_{\Delta \hat{x}}^{-1})$ are the smallest and largest eigenvalues of $R_{\Delta \hat{x}}^{-1}$, to get the following upperbound on the 'position error' and 'no position error' probabilities:

$$P_{pos\_error} \leq P(\left\| \Delta \hat{\vec{x}}_{LS} \right\|_{R_{\Delta \hat{x}}^{-1}}^2 > \lambda_{\min}(R_{\Delta \hat{x}}^{-1}) \cdot RNP_{\Delta \hat{x}}^2) \quad (4.2.6)$$

$$1 - P_{pos\_error} \leq P(\left\| \Delta \hat{\vec{x}}_{LS} \right\|_{R_{\Delta \hat{x}}^{-1}}^2 < \lambda_{\max}(R_{\Delta \hat{x}}^{-1}) \cdot RNP_{\Delta \hat{x}}^2) \ (4.2.7)$$

in which the normalized position error has a noncentral chi-square distribution

$$\left\| \Delta \hat{\vec{x}}_{LS} \right\|_{R_{\Delta \hat{x}}^{-1}}^2 = \Delta \hat{\vec{x}}_{LS}^T R_{\Delta \hat{x}}^{-1} \Delta \hat{\vec{x}}_{LS} \sim \chi^2(m, \lambda_{\Delta \hat{x}}) \qquad (4.2.8)$$

with noncentrality

$$\lambda_{\Delta \hat{x}} = \vec{\mu}_{\Delta \hat{x}}^T R_{\Delta \hat{x}}^{-1} \vec{\mu}_{\Delta \hat{x}} = \vec{\mu}_{\nu}^T N^T R_{\Delta \hat{x}}^{-1} N \vec{\mu}_{\nu} \qquad (4.2.9)$$

Advantage of this approximation is, that it always stays on the 'safe side', unlike the approximation of Lee. Because it uses spheres, or, in two dimensions, circles, we will refer to it as the 'circle approximation' in the remainder of this paper.

4.3 Missed and false detection probabilities

This section will explain how the probabilities of missed and false detection can be computed. We have showed that the distributions of the position error and the test statistic both contain an unknown measurement bias. Therefore, we can only start computing after having made the following assumptions on that bias:

- during normal system operation all measurements are unbiased, that is, $\vec{\mu}_{\nu} = \vec{0}$
- when satellite i is in error, the corresponding element of $\vec{\mu}_{\nu}$ can have any value
- the probability that a satellite is in error in a certain sample (P_S) is known

For simplicity we will assume that at most one measurement is biased simultaneously. However, the concept that is discussed can be applied equally well in the multiple failure case, see [Ober96a][Ober96b]. Because we assume that at most one measurement is biased, a sample can contain either zero or one biased measurement. The probabilities of missed and false detection are nothing but the sum of the missed and false detection probabilities under the zero and one bias case:

$$P_{MD} = P_{MD}^0 + P_{MD}^1 \qquad (4.3.1)$$
$$P_{FD} = P_{FD}^0 + P_{FD}^1 \qquad (4.3.2)$$

These probabilities can be written as the product of the occurrence of the zero or one bias case and the conditional probability that a missed or false detection results:

$$P_{MD}^0 = P_{no\_bias} \cdot P_{MD|no\_bias} \qquad (4.3.4)$$

$$P_{MD}^1 = \sum_{i=1}^{n} P_{bias\_i} \cdot P_{MD|i} \qquad (4.3.5)$$

$$P_{FD}^0 = P_{no\_bias} \cdot P_{FD|no\_bias} \qquad (4.3.6)$$

$$P_{FD}^1 = \sum_{i=1}^{n} P_{bias\_i} \cdot P_{FD|i} \qquad (4.3.7)$$

in which the following notations are introduced:

$P_{MD|i}$: conditional probability of missed detection when measurement i is biased

$P_{FD|i}$: conditional probability of false detection when measurement i is biased

$P_{MD|no\_bias}$: conditional probability of missed detection when no measurement is biased

$P_{FD|no\_bias}$: conditional probability of false detection when no measurement is biased

P_{no_bias}: probability that no measurement is biased

P_{bias_i}: probability that measurement i is biased

The probabilities that a sample contains no biases, or a bias in measurement i, are a function of the probability of a satellite failure P_S and the number of measurements n:

$$P_{bias\_i} = P_S (1 - P_S)^{n-1} \qquad (4.3.8)$$

$$P_{no\_bias} = (1 - P_S)^n \qquad (4.3.9)$$

and are therefore assumed to be known. In case of no bias, the distribution of position error and test statistic are fully known as well, and the computation of $P_{MD|no\_bias}$ and $P_{FD|no\_bias}$ is straightforward. Because no information is available on the behavior of erroneous satellites, we do not know anything, not even statistically, about the size of occurring biases. The only thing we can do is to assume that this bias has the 'worst possible size', that leads to the highest probabilities of missed and false detection. The next section explains how this approach can be applied.

4.3.1 Computing worst case probabilities

We will now discuss the computation of the worst case measurement biases that maximize the probability of either missed or false detection ($P_{MD|i}$ or $P_{FD|i}$).

We consider the case in which the ith measurement is biased. The measurement bias will then have the following form:

$$\vec{\mu}_v^{(i)} = [0 \cdots 0 \quad \underset{i}{\mu_i} \quad 0 \cdots 0]^T \qquad (4.3.1.1)$$

in which μ_i is unknown.

The measurement bias influences the noncentralities of the distributions of both the test statistic and position error (or its normalized version (4.2.8)). It is important to see that the ratio between these two noncentralities is independent of μ_i:

$$ratio(i) = \frac{\lambda'_{\Delta\hat{x}}(\vec{\mu}_v^{(i)})}{\lambda_{SSE}(\vec{\mu}_v^{(i)})} = \frac{(N^T N)_{ii}}{(D^T R_v^{-1} D)_{ii}} \qquad (4.3.1.2)$$

in which the noncentralities are just the ones from (4.2.3) and (4.1.2) with their dependence on the measurement bias made explicit. This ratio measures the coupling between position error and test statistic: the smaller the ratio, the better the test statistic represents the error in the position.

Figure 4 shows how (4.3.1.2) can be interpreted as the slope of the square position error plotted against the test statistic *in the noiseless case*. When noise is added, we get a scattered cloud that describes the stochastic relation between test statistic and position error for a certain measurement bias.

As becomes clear from the figure, a large ratio gives a large probability of missed detection, while a small ratio implies a large probability of false alarm. These probabilities will also depend on the size of the measurement bias. Because this size is unknown, we will have to take a worst case approach. The worst case value of μ_i will depend on all of the following parameters:

- the threshold of the test statistic $SSE_{threshold}$
- the allowed position error $RNP_{\Delta\hat{x}}$
- the noise covariance matrix R_v (quality and number of measurements)
- the ratio (4.3.1.2)

Unfortunately, the worst case value can generally not be found analytically, and will have to be computed iteratively by maximizing $P_{MD|i}$ and $P_{FD|i}$ explicitly as a function of μ_i.

4.4 Navigational practice

In this section, we will shortly discuss the conventional way of looking at RAIM/AAIM algorithms. In 4.4.1 we will illustrate the way performance of RAIM/AAIM is often computed by measuring error detection power in the measurement rather than the position domain. Section 4.4.2 describes how the measurement geometry is generally represented by one scalar integrity metric instead of the *n* different ratios (4.3.1.2).

4.4.1 The measurement bias formulation

In much of the navigation literature [Leva96], RAIM and AAIM performance are computed using a measurement bias detection formulation

$$H_0\,(no\;error):\;\vec{\mu}_v = \vec{0}$$
$$H_1\,(error):\;\;\;\;\vec{\mu}_v \neq \vec{0} \tag{4.4.1}$$

rather than the position error formulation from (4.1).

Based on (4.4.1) the probability of missed detection is often defined as the probability of an undetected *measurement bias* rather than that of the unallowable position error of (4.1). The norm of the bias is taken such, that the resulting position bias equals $RNP_{\Delta\hat{z}}$. In figure 5, we have indicated the missed detection probability that is obtained by $P_{MD,conv}$. The false detection probability $P_{FD,conv}$ is defined as the probability that a detection occurs while $\vec{\mu}_v = \vec{0}$.

It is hard to say beforehand whether $P_{MD,conv}$ is an under- or an overestimation of P_{MD}. In figure 5, we can see that for a given measurement bias only part of the area of $P_{MD,conv}$ falls into the missed detection region. Because not every undetected measurement bias will cause an unallowable position error, $P_{MD,conv}$ could be considered to be too conservative. On the other hand, the size of the measurement bias that is chosen to determine $P_{MD,conv}$ is usually larger than the 'worst case' measurement bias as discussed in section 4.3, as was already reported in [Lee95]. Therefore, it is just as well possible that $P_{MD,conv}$ is an *underestimation* of the *worst case* missed detection probability. For $P_{FD,conv}$, similar arguments hold.

Note that the definition of $P_{MD,conv}$ implicitly assumes that no missed detections occur when no bias is present. In our original notation, this assumption looks like:

$$P_{MD}^0 << P_{MD}^1 \tag{4.4.2}$$

This assumption will only be valid when the accuracy is much higher than the allowed position error. However, when the position solution and test statistic are more noisy, the missed detection probability under unbiased operation might not always be negligible. A similar assumption is made in the traditional definition of the false detection probability; false detections are assumed to occur only when there are no measurement biases:

$$P_{FD}^1 << P_{FD}^0 \tag{4.4.3}$$

As can be seen from (4.3.6) and (4.3.7), this is only true when the probability of bias-occurrence is much lower than the false alarm probability with no biases present ($P_{bias\_i} << P_{FD|no\_bias}$).

4.4.2 Representing measurement geometry by a scalar integrity metric

Of all parameters that influence the worst case value of a measurement bias, only the ratio (4.3.1.2) differs for different measurements. To simplify the use of geometrical considerations, the geometry is often described only by the worst case ratio over all measurements, rather than by all ratios separately. When considering missed detection probabilities, this leads to the use of the following metric of integrity, called the Bias Integrity Threat [Ober96b]:

$$BIT = \max_i ratio(i) \tag{4.4.2.1}$$

which is similar to the well known integrity DOP (δH_{max}) when all measurements have the same standard deviation.

Although to the best knowledge of the author this has not been done before, we could define a similar metric to represent the worst case influence of geometry on the probability of false alarm. We will call this metric the Bias Alarm Threat:

$$BAT = \min_i ratio(i) \tag{4.4.2.2}$$

When we represent the geometry by the worst case measurement only, we have to compute the worst case $P_{MD|i}$ and $P_{FD|i}$ only for the measurement with the highest and lowest ratio respectively. When the measurement with the highest ratio has index *hi*, and the one with the lowest ratio index *li*, this simplification provides the following upperbounds on (4.3.5) and (4.3.7):

$$P_{MD}^1 \leq n \cdot P_{bias\_i} \cdot P_{MD|hi} \tag{4.4.2.3}$$
$$P_{FD}^1 \leq n \cdot P_{bias\_i} \cdot P_{FD|li} \tag{4.4.2.4}$$

in which $P_{MD|hi}$ is a function of the *BIT*, and $P_{FD|li}$ a function of the *BAT*. Obvious advantage of this approach is that the search for the 'worst case' bias size has to be

performed only once. A disadvantage is the loss of availability due to the overestimation of the missed and false detection probabilities.

5. Computations

Having described the ins and outs of the ways to compute RAIM/AAIM performance in the position domain, we will now present the results of some computations that were done with actual GPS constellations. These computations investigate the accuracy of the discussed position error approximations and the effect they have on the resulting missed and false detection probabilities. They also examine the correctness of the conventional approach from section 4.4.

More in particular, the computations are designed to give insight in:

- The difference between the exact worst case missed and false detection probabilities and those obtained using:
  1. The circle approximation (position error only)
  2. Lee's approximations (for both position error and test statistic)
  3. The conventional approach
- The effect of representing the measurement geometry by the worst integrity measurement only
- The validity of the assumption that the probability of missed detection in the no bias case is negligible
- The validity of the assumption that the probability of false detection in the case of biases is negligible
- The optimality of the conventional way of choosing a threshold for the test statistic

We consider navigation with GPS only, and assume that the probability that a satellite is in error in a certain sample equals [Shively93]

$$P_S = 1.27 \cdot 10^{-8} \cdot T_{sample} \cdot \text{s}^{-1} \qquad (5.1)$$

in which T_{sample} is the time between two decisions. In the simulations we will take the following values, corresponding to the RNP requirements for aircraft nonprecision approach [Graas96]:

$$T_{sample} = 10 \text{ s}$$
$$RNP_{\Delta \hat{x}} = 555 \text{ m}$$

The standard deviation of the measurements is 33 m.

An exact, optimal choice of $SSE_{threshold}$ is very hard to find. If we would like to have a constant probability of false or missed detection, this would mean that we have to fix a sum of $n+1$ probabilities that all depend on both the threshold and the geometry. In this paper, we will not bother with optimal threshold selection, and just take the thresholds as they are conventionally determined by fixing $P_{FD,conv}$ (see section 4.4.1 and figure 5). Unfortunately, due to a problem in the software, the used threshold varied with the number of satellites in the computation, see table 5.1. Although this influences the absolute values of the probabilities that are computed, we don't expect this problem to have a major impact on the comparison of the different methods.

In all computations, we look at GPS constellations that occur at 4 large European Airports: Amsterdam, London, Frankfurt and Rome, taking a sample every 15 minutes during 24 hours. All computations are performed with an accuracy of 10^{-10}. Therefore, we exclude samples with missed or false detection probabilities that are smaller than 5×10^{-10} from the figures that are presented. We consider the detection of horizontal position errors only.

5.1 Comparison of position error approximations

First of all, we have investigated the two position error probability approximations of section 4.2 for biases of known size. In each constellation, the satellite with the worst integrity (largest ratio (4.3.1.2)) has been given three different biases, causing position errors of 400, 550 and 650 meters respectively. We have computed exact and approximated probability of a position error for these three cases. The result are given in table 5.1.1, from which we can draw the following conclusions:

- Both approximations are becoming better when the position bias grows
- The 'circle method' always overestimates the position error probability, and overestimates grossly for small position biases with a very small position error probability
- Lee's method always underestimates the position error probability slightly

In section 5.3 the effect of the position error approximations on the missed and false detection probabilities will be further investigated.

	$P_{FD,conv}$
5 satellites	5.5×10^{-5}
6 satellites	9.8×10^{-5}
7 satellites	13×10^{-5}
8 satellites	16×10^{-5}

Table 5.1. $P_{FD,conv}$ values on which $SSE_{threshold}$ is based

5.2 Assumptions on the causes of missed and false detections

As we have seen in section 4.4.2, it is often assumed that missed detection are always caused by measurement biases, and never by noise only. Likewise, false detections are supposed to happen only when there are no measurement biases. The validity of these two assumptions is investigated in sections 5.2.1 and 5.2.2.

5.2.1 Missed detections only occur when there are biases

In table 5.2.1.1 we present the contribution of the probability of missed detection under the no bias case (P_{MD}^0) to the total probability ($P_{MD}^0 + P_{MD}^1$). As we can see, this contribution is generally very small, but in the 5 satellite case, situations occur in which P_{MD}^0 even dominates. In these cases, GPS was not meeting the accuracy requirements, and should have been considered 'not available'. We therefore conclude that the assumption is valid for the parameter values that were used, as long as GPS performs within the required accuracy.

5.2.2 False detections only occur when there are no biases

Table 5.2.1.1 also shows the percentage of the contribution of the probability of false detection in the one bias case (P_{FD}^1) to the total probability ($P_{FD}^0 + P_{FD}^1$). As we can see, this contribution is very small in all cases, and the assumption that it is negligible seems valid for the used parameter values. We have observed that in the case of a bias, the conditional false detection $P_{FD|i}$ becomes close to one for most of the satellites, except for those with a very high ratio (4.3.1.2). We can thus conclude that the occurrence of a bias is just too unlikely to reveal this high value of $P_{FD|i}$ in the total false detection probability.

5.3 Comparison of maximum missed and false detection probabilities

We will now examine the missed and false detection probabilities from (4.3.1) and (4.3.2). We compute both exact and approximated maximum false and missed detection probabilities, using the position error approximations and the conventional method. It should be noted that in all cases, we consider each satellite separately. The effects of using the 'worst integrity' satellite only will be discussed in section 5.4.

Because a strong influence of the number of available satellites is to be expected, we have used 'best accuracy' subconstellations of 5, 6 and 7 satellites, instead of the all in view constellation. Table 5.3.1 and 5.3.2 show the results. They give probability ratios of all approximated probabilities and their exact counterparts. A ratio larger than one corresponds to an overestimation, a ratio smaller than one to an underestimation of the exact value.

We can conclude that:

- The circle method always overestimates the worst case missed detection probability P_{MD}, sometimes largely when only 5 or 6 satellites are in view
- The results that Lee obtains are generally quite accurate, but a few gross underestimations of P_{MD} occur for the 5 satellites case
- The conventional approach always overestimates the worst case P_{MD}
- Both the circle and the conventional method get accurate results for the worst case false detection probability P_{FD}, but a few gross underestimations of P_{MD} occur with 5 satellites in view
- Lee's method underestimates P_{FD}, and this gets worse for an increasing number of satellites
- The selected threshold is accurate

Lee's method gives good results for the missed detection probability only. It always underestimates the position error probability, but overestimates the 'no detection' probability, giving a rather accurate product most of the time. P_{MD}^0 is underestimated largely, but dominates only in a few samples (see section 5.2). For these samples the conventional method, that completely ignores P_{MD}^0, gives large underestimations as well. For the false detection case, the underestimated detection probability is not sufficiently compensated by the overestimated 'no position error' probability, that has very small absolute values, and too low false detection probabilities are obtained as a result.

The results of this section have an important implication: due to the overestimation of the missed detection probability in the conventional approach, RAIM/AAIM availability studies based on this approach are generally too pessimistic. As we will show in the next section, the custom to represent geometry by the worst integrity

satellite tends to give an even stronger overestimation of P_{MD}.

5.4 Effect of using worst integrity satellite only

To see what is the influence of using only the worst integrity satellite ('worst' in terms of probability of missed detection probability of a bias on that satellite) in order to simplify computations, as discussed in section 4.4.2, we have compared the upperbound (4.4.2.3) to the exact missed detection probability, under the assumption of the occurrence of a bias. The results are summarized in table 5.4.1. The entries of this table lie between one and the number of satellites n: a one indicates an equal contribution to P_{MD}^1 of each satellite, an n means that only one single satellites contributes significantly.

We can conclude the following:

- The less satellites are available, the better the upperbound fits the exact value of the missed detection probability, due to the fact that multiple satellites contribute substantially to P_{MD}
- In the case of 7 satellites, only the worst case integrity satellite contributes significantly
- An increase in availability is to be expected when we compute missed detection probabilities $P_{MD/i}$ for every satellite instead of using the 'worst integrity' satellite only

Table 5.4.2 gives the overestimation factors that are found with the conventional method combined with using only the worst integrity satellite, incorporating both of the effects discussed in section 4.4. It makes clear that conventional performance computations give highly pessimistic values for missed detection probabilities, and therefore for RAIM availability, and they will label certain constellations 'unavailable' while both missed and false detections are sufficiently small. The only cases in which they give an underestimation are the ones in which there is insufficient position accuracy.

6. Conclusions and recommendations

In this paper, we have shown how to compute the performance of RAIM in the position domain, and compared this performance to the one obtained with the conventional measurement domain based method.

Computations for GPS show that the conventional method:

1. overestimates the missed detection probability in case of a bias in a certain measurement

2. often represents geometry by the worst integrity measurement only, instead of all measurements separately, leading to an even larger overestimation of the missed detection probability

Both effects lead to a decreased RAIM availability. Availability can be improved easily by using the bias detection probability on a per measurement basis, rather than just using the 'worst integrity' measurement only. It will be more difficult to exploit the advantages of exact position domain computations, because the computation of exact missed and false detection probabilities is very time consuming. The approximations that were discussed in this paper are either inaccurate or possibly underestimating, and closer and computationally efficient upperbounds should be found in order to take full advantage of the insights provided in this paper.

REFERENCES

[Brown96] Brown, R.G.; "Receiver Autonomous Integrity Monitoring", in *Global Positioning System: theory and applications Volume 2*, eds. B.W. Parkinson and J.J. Spilker Jr., American Institute of Aeronautics and Astronautics, 1996

[Graas96] Graas, F. van; "Signals Integrity", AGARD Lectures Series No. 207, Systems Implications and Innovative Application of Satellite Navigation, 1-12 July 1996

[Johnson72] Johnson, N.L. and S. Kotz; "Continuous Univariate Distributions", volume 1, first edition, John Wiley & Sons Inc., 1972

[Lee95] Lee, Y.C; "New techniques relating fault detection and exclusion Performance to GPS Primary Means Integrity Requirements", The 8th international technical meeting of the ION, September 1995

[Lee96] Lee, Y.C., K. Van Dyke, B. DeCleene, J. Studenny and M. Beckmann; "Summary of RTCA SC-159 GPS Integrity Working Group Activities", Proceedings of the National technical meeting of the ION, January 1996

[Leva96] Leva, J.L., M. Uijt de Haag and K. Van Dyke; "Performance of Standalone GPS", *in Understanding GPS: Principles and Applications*, Edited by E.D. Kaplan, Artech House, 1996

[Ober96a] Ober, P.B.; "Integrity Monitoring: information paper", TVS memorandum REP9606B, , Delft University of Technology, Faculty of Electrotechnics, TVS Group, June 1996

[Ober96b] Ober, P.B.; "New, Generally Applicable Metrics for RAIM/AAIM Integrity Monitoring", proceedings of ION GPS-96, 1996

[Rao95] Rao, C.R. and H. Toutenburg; "Linear Models: least squares and alternatives", Springer, 1995

[Ruben62] Ruben, H.; "Probability content of regions under spherical normal distributions 4: the distribution of homogeneous and non-homogeneous quadratic functions of

normal variables", Annals of Math. Statistics Volume 31, pp. 542-570, 1962

[Shively93] Shively, C.; "Satellite Criticality Concepts for Unavailability and Unreliability of GNSS Satellite Navigation", Navigation, Vol. 40, Number 4, pp. 429-450, Winter 1993

[Tong90] Tong, Y.L.; "The multivariate normal distribution, Springer Verlag New York, 1990

Appendix A. Independence of position error and test statistic

The position error and the test statistic are distributed independently. This can be shown as follows. In [Johnson72], it is proved that when $\vec{v}$ is normally distributed

$$\vec{v} \sim \mathsf{N}\,(\,\vec{\mu}_v, R_v\,) \tag{A.1}$$

two quadratic forms $\vec{v}^T A \vec{v}$ and $\vec{v}^T B \vec{v}$ (A and B positive semi-definite) are independent if and only if

$$R_v A R_v B R_v = 0 \tag{A.2}$$

The position error and test statistic are two examples of such quadratic forms with

$$A = N^T N \tag{A.3}$$
$$B = D^T R_v^{-1} D \tag{A.4}$$

We just have to substitute (A.3) and (A.4) in (A.2) to get the following sufficient condition for their independence:

$$R_v N^T N R_v D^T R_v^{-1} D R_v = 0 \tag{A.5}$$

which is fulfilled because

$$
\begin{aligned}
NR_v D^T &= \\
&= (H^T R_v^{-1} H)^{-1} H^T R_v^{-1} \cdot R_v \cdot (I - R_v^{-1} H (H^T R_v^{-1} H)^{-1} H^T) \\
&= (H^T R_v^{-1} H)^{-1} H^T - (H^T R_v^{-1} H)^{-1} H^T \\
&= 0
\end{aligned} \tag{A.6}
$$

Appendix B. The distribution of quadratic forms in normal variables

In [Johnson72] the distribution of general quadratic forms in normal variables is discussed. Although we can not go into much detail here, we will indicate shortly how the computation of the distribution function can be done. Johnson shows, that the distribution function of a quadratic form in n normal variables

$$Q = \vec{v}^T A \vec{v} \ \text{ with } \ \vec{v} \sim \mathsf{N}\,(\,\vec{\mu}_v, R_v\,) \tag{B.1}$$

with A positive semi-definite, can be computed as a sum of chi-square distribution functions:

$$P(Q < Q_{\lim}) = \sum_{j=0}^{\infty} e_j P\left(\chi^2(n+2j) < \frac{Q_{\lim}}{\beta} \right) \tag{B.2}$$

for some suitably chosen constant β. Expressions for the coefficients e_j and for β can be found in [Johnson72] and [Ruben62]. These references also provide upperbounds of the error that is made when the series from (B.2) is truncated. Because different chi-square distribution functions are used in each of the terms of (B.2), that each have to be computed by a series expansion as well, computation is very involved.

	P_{pos_error} Exact	P_{pos_error} Circle	P_{pos_error} Lee
450 m	0.00014	0.115	0.00011
550 m	0.440	0.897	0.433
650 m	0.995	0.999	0.995

Table 5.1.1 Mean values of the exact and approximated position error probabilities as a function of the position bias

	$P_{MD}^0/(P_{MD}^0 + P_{MD}^1)$			$P_{FD}^1/(P_{FD}^0 + P_{FD}^1)$		
	min	mean	max	min	mean	max
5 sats	0	0.0075	0.9833	0.0048	0.0097	0.0114
6 sats	0	0	0.0013	0.0061	0.0075	0.0077
7 sats	0	0	0	0.0063	0.0066	0.0067

Table 5.2.1.1 The contributions of missed detections occurring when there is no bias, and of false detections occurring when there is, to the total missed and false detection probabilities

	$(P_{MD}^0 + P_{MD}^1)$ circle / $(P_{MD}^0 + P_{MD}^1)$ exact			$(P_{MD}^0 + P_{MD}^1)$ Lee / $(P_{MD}^0 + P_{MD}^1)$ exact			$P_{MD,conv}$ / $(P_{MD}^0 + P_{MD}^1)$ exact		
	min	mean	max	min	mean	max	min	mean	max
5 sats	1.0000	2.1797	20.2616	0.0167	0.9895	1.1854	0.0201	1.3050	2.3349
6 sats	1.0005	2.4540	17.0038	1.0005	1.1297	1.2563	1.0004	1.5386	1.9871
7 sats	1.3817	1.8326	2.2320	1.3469	1.3996	1.5020	1.8912	1.9492	1.9851

Table 5.3.1 The ratios of approximated and exact worst case missed detection probabilities, computed with the circle and Lee's approximation and with the conventional method respectively

	$(P_{FD}^0 + P_{FD}^1)$ circle / $(P_{FD}^0 + P_{FD}^1)$ exact			$(P_{FD}^0 + P_{FD}^1)$ Lee / $(P_{FD}^0 + P_{FD}^1)$ exact			$P_{FD,conv}$ / $(P_{FD}^0 + P_{FD}^1)$ exact		
	min	mean	max	min	mean	max	min	mean	max
5 sats	1.0000	1.0005	1.0050	0.5024	0.5049	0.5057	0.9886	0.9903	0.9952
6 sats	1.0000	1.0001	1.0016	0.0940	0.0953	0.0955	0.9923	0.9925	0.9939
7 sats	1.0000	1.0000	1.0004	0.0283	0.0288	0.0288	0.9933	0.9934	0.9937

Table 5.3.2 The ratios of approximated and exact worst case false detection probabilities, computed with the circle and Lee's approximation and with the conventional method respectively

	P_{MD}^1 worst sat only / P_{MD}^1 exact		
	min	mean	max
5 sats	2.5122	4.6332	5.0000
6 sats	3.4533	5.8181	6.0000
7 sats	7.0000	7.0000	7.0000

Table 5.4.1 The ratio of the missed detection probability using the worst integrity satellite only, and the exact value (in case of a bias)

	$P_{MD,conv}$ worst sat only / $(P_{MD}^0 + P_{MD}^1)$ exact		
	min	mean	max
5 sats	0.0593	5.9696	9.9171
6 sats	5.9755	8.8876	11.8348
7 sats	13.2383	13.6446	13.8959

Table 5.4.2 The ratio of the missed detection probability using the worst integrity satellite only and the conventional method, and the exact value
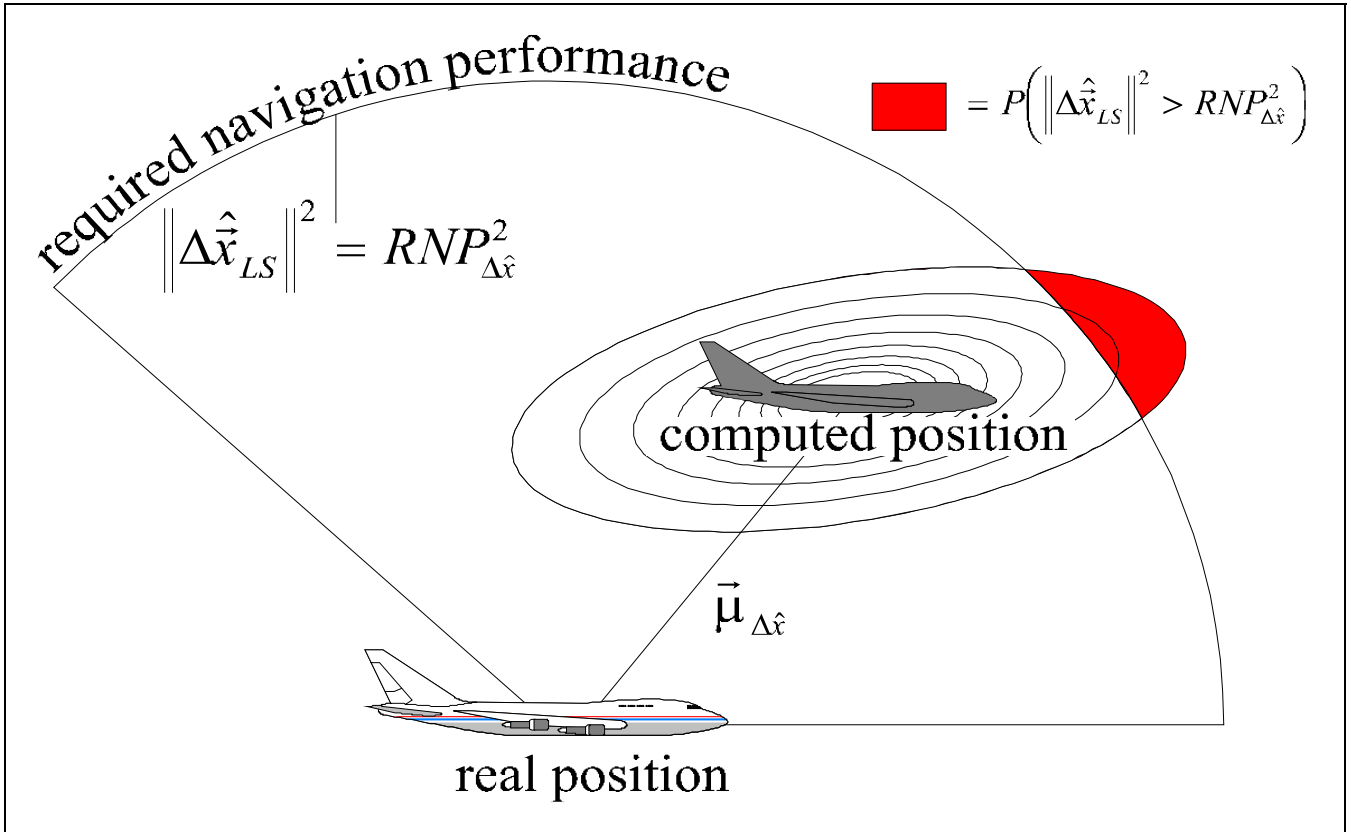
Figure 1. The position error probability is the probability content of an elliptically contoured distribution outside the error region that is allowed by the required navigation performance parameters
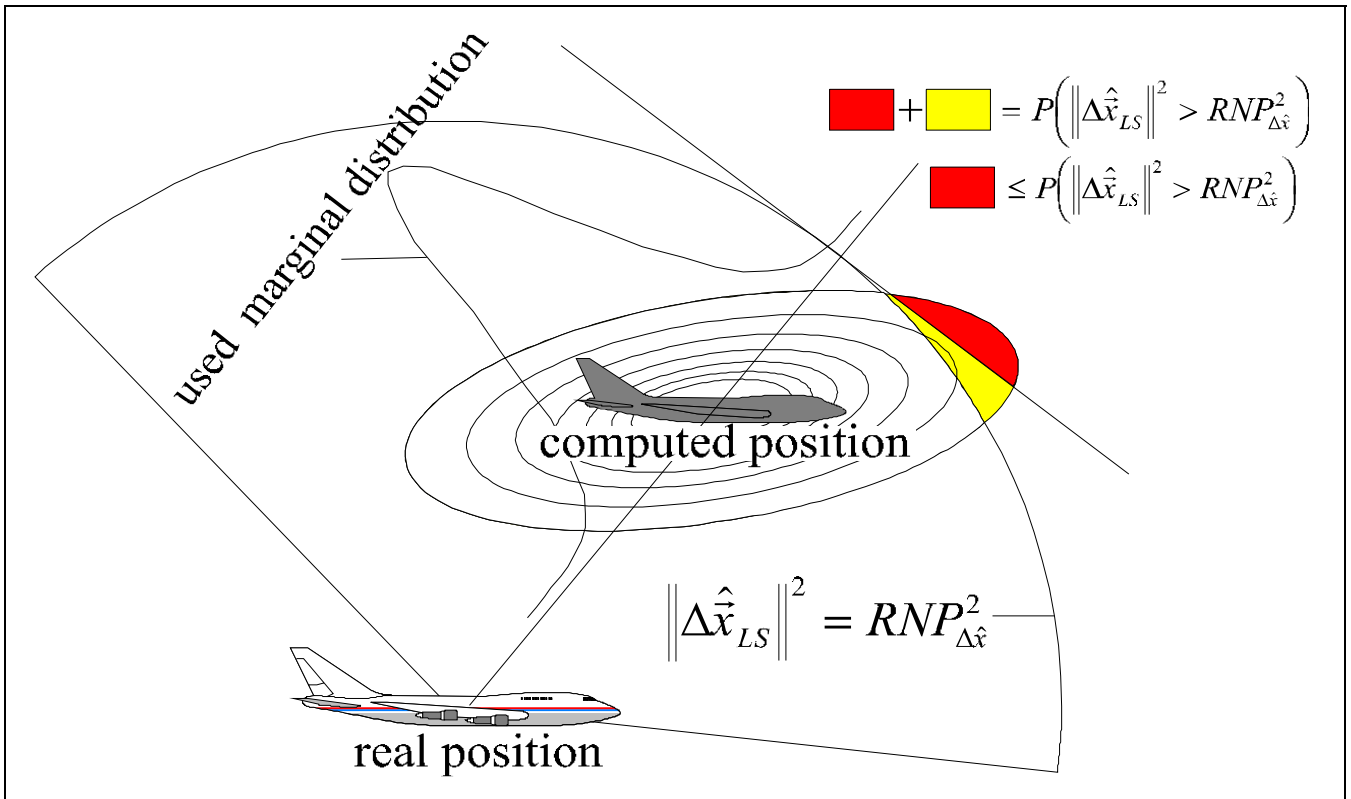
Figure 2. The position error probability as estimated by Lee (dark area). Clearly, this is always an underestimation of the actual probability (dark and light area).
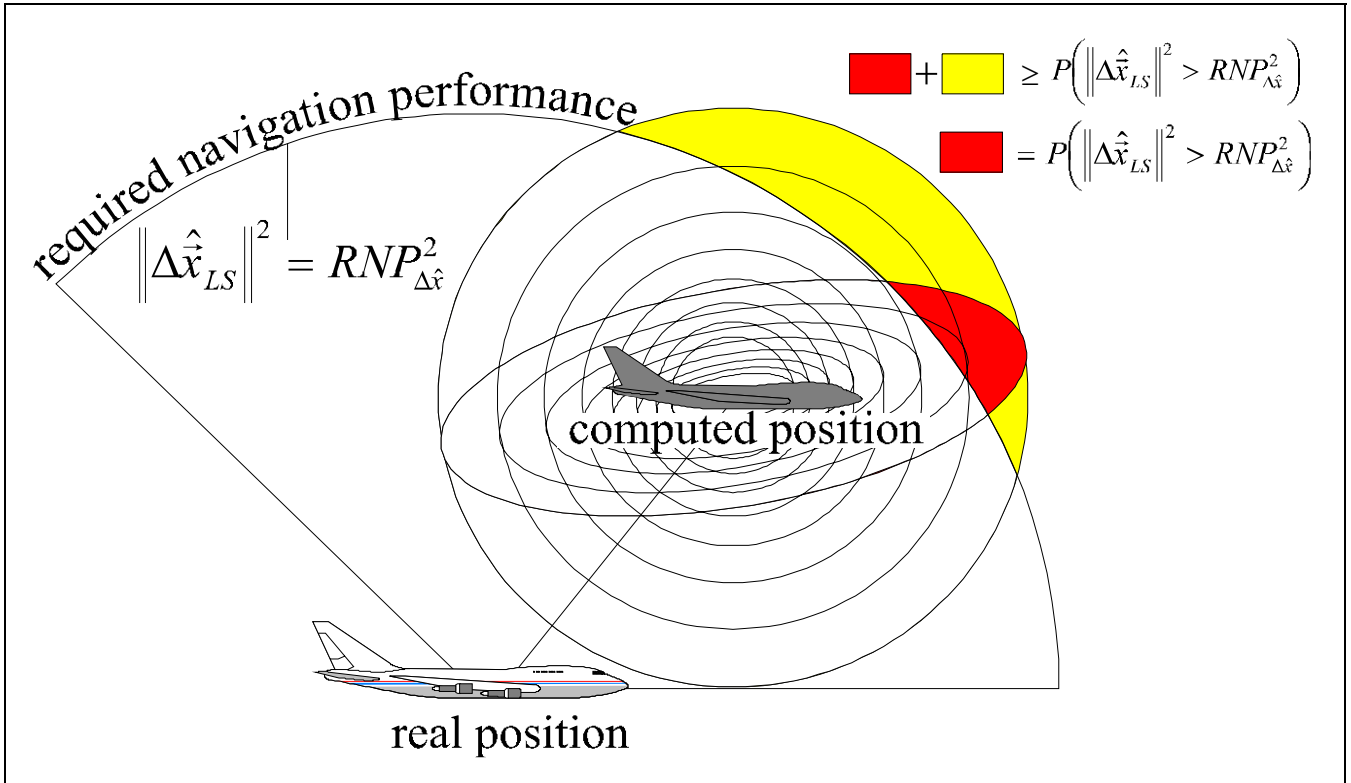
Figure 3. An upperbound on the position error probability can be found by using the circle-shaped areas of the distribution of the normalized position error, instead of the ellipses of the distribution of the position error.
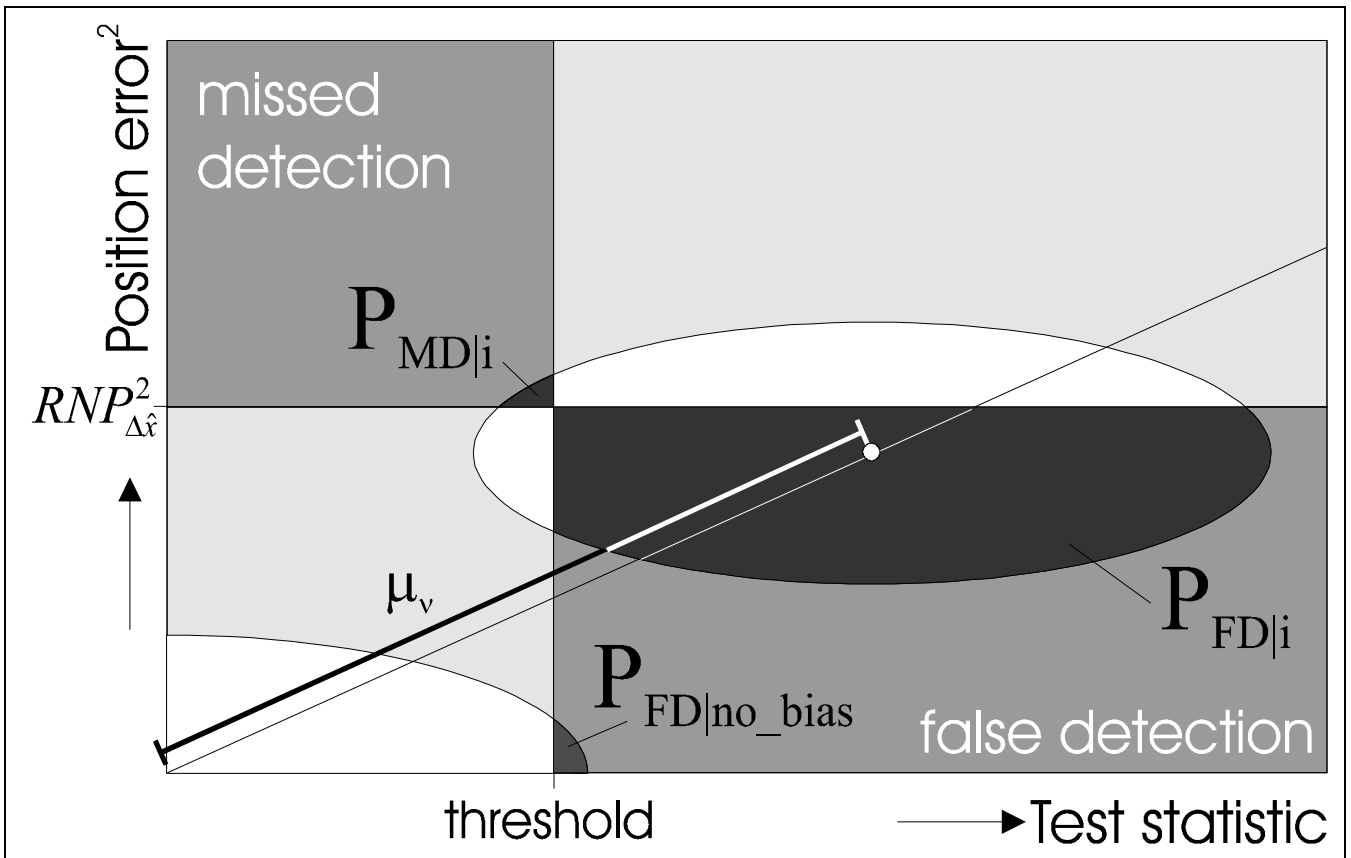
Figure 4. The probabilities of false and missed detection depend on the size of the measurement bias and of the slope of the relation between position error and test statistic.
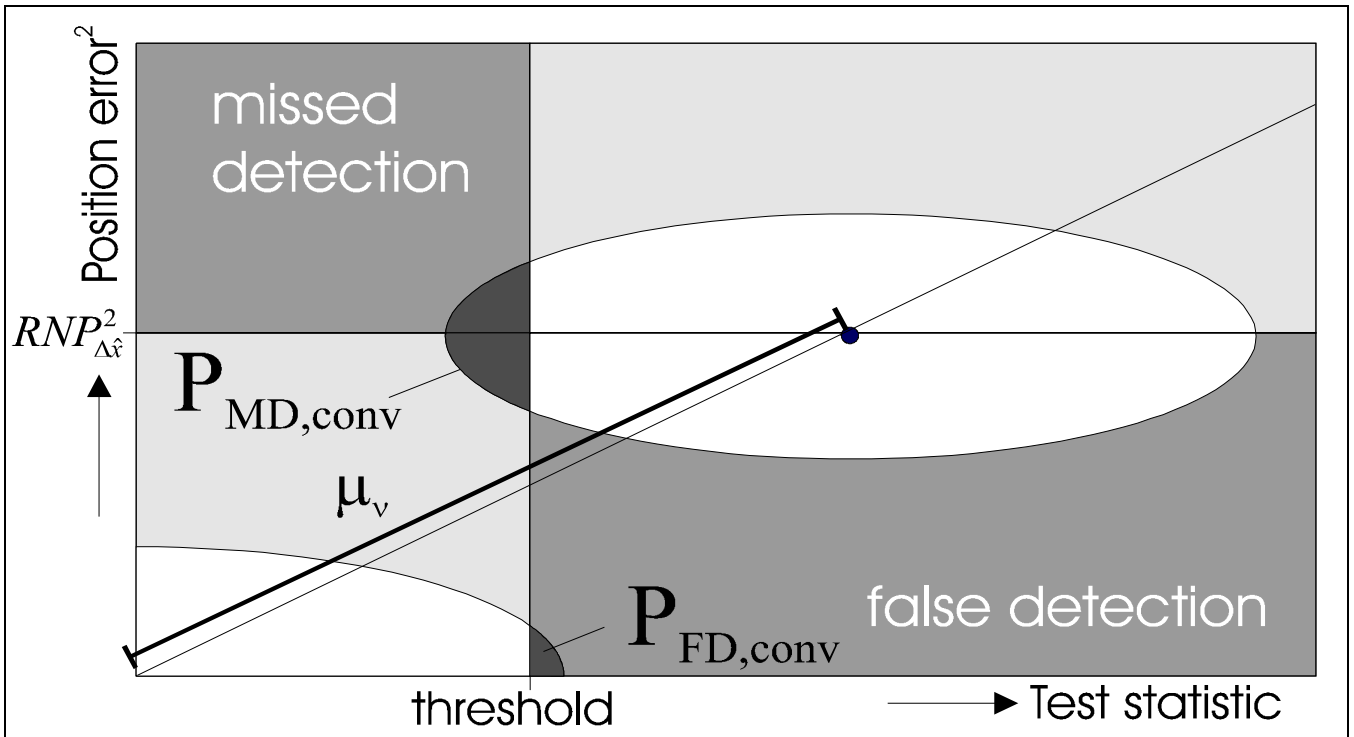
Figure 5. The conventional way of defining the probabilities of false and missed detection. False detection are detections generated when there is no position bias, missed detections occur when there is a measurement bias but no detection.